Probabilistic quantum gates between remote atoms through interference of optical frequency qubits

L.-M. Duan, M. J. Madsen, D. L. Moehring, P. Maunz, R. N. Kohn, Jr., and C. Monroe

FOCUS Center and Michigan Center for Theoretical Physics, Department of Physics, University of Michigan, Ann Arbor, Michigan 48109, USA

We propose a scheme to perform probabilistic quantum gates on remote trapped atom qubits through interference of optical frequency qubits. The method does not require localization of the atoms to the Lamb-Dicke limit, and is not sensitive to interferometer phase instabilities. Such probabilistic gates can be used for scalable quantum computation.

PACS number(s): 03.67.Lx, 03.67.Hk, 42.50.−p

Entangled quantum states, at the heart of quantum-information processing, are notoriously difficult to generate and control. Generating entangled states becomes dramatically simpler when the entanglement operations are allowed to succeed with only a finite (perhaps small) probability, as long as it is known when the operations succeed [1–5]. If entangling *gates* can be implemented in such a probabilistic fashion, it has recently been shown that scalable quantum computation is still possible, no matter how small the gate success probability [6,7]. Compared with deterministic gates, the additional overhead in resources (such as the number of qubit manipulations) for probabilistic quantum computation scales only polynomially with both the size of the computation and the inverse of the gate success probability [6].

There have been recent proposals for implementation of probabilistic gates [7–9], using atomic qubits inside optical cavities. In this paper, we propose a scheme for probabilistic quantum gate operations that act on trapped atoms or ions in free space (with or without cavities). Compared with previous methods, this scheme has two outstanding features. First, optical frequency qubits are used to connect and entangle matter qubits at distant locations. The two states comprising this optical qubit have the same polarization, but differ in frequency by the atomic qubit splitting (typically in the microwave region for hyperfine atomic qubits). These closely spaced frequency components have basically zero dispersion in typical optical paths; thus this optical qubit is highly insensitive to phase jitter inherent in optical interferometers. Such optical frequency qubits have been demonstrated in a very recent experiment [10], through control of a trapped cadmium ion with ultrafast laser pulses. Second, the proposed entangling scheme does not require localization of the atoms to the Lamb-Dicke limit. Motion of the atomic qubits can be larger than the optical wavelength. Although ions can be localized well under the Lamb-Dicke limit through laser cooling in a strong trap, the elimination of this stringent requirement should greatly simplify experiments. This is particularly important for ions confined in miniature electrode structures fabricated on a chip [11,12], where ion heating may become more significant [13]. This feature is also crucial for neutral atom qubits, where confinement to the Lamb-Dicke regime is very difficult.

Our scheme is illustrated in Fig. 1. The qubit is represented by two $S_{1/2}$ ground-state hyperfine levels of an alkali-metal-like atom (ion), with $|0\rangle \equiv |F, m=0\rangle$ and $|1\rangle \equiv |F+1, m=0\rangle$. These "clock" states are particularly insensitive to stray magnetic fields. In the figure, for simplicity, we take $F=0$, which is the case for ions such as ^{111}Cd$^+$, but the scheme works for any value of F. To perform a probabilistic gate on two remote atoms 1 and 2, we first excite both of the atoms to the $P_{1/2}$ excited electronic state with a π-polarized ultrafast laser pulse [14]. We assume the laser has a bandwidth that is larger than the hyperfine splitting (14 GHz for ^{111}Cd$^+$), but smaller than the fine-structure splitting between $P_{1/2}$ and $P_{3/2}$ (74 THz for ^{111}Cd$^+$). Typical picosecond pulses used in experiments (bandwidth $\sim$500 GHz) satisfy these requirements [10]. Under the above condition, we can assume the pulse only drives the $D1$ transition from the ground state $S_{1/2}$ to the excited state $P_{1/2}$ [15]. Due to dipole selection rules, for a π-polarized pulse, only the hyperfine transitions $|F, m=0\rangle \rightarrow |F'+1, m=0\rangle$ and $|F+1, m=0\rangle \rightarrow |F', m=0\rangle$ are allowed, where the upper hyperfine spin $F'=F$. Thanks to the selection rules, each qubit state is transferred to a unique excited hyperfine level after the pulsed laser excitation. This point is critical for successful gate operation.

After this laser excitation, the atoms eventually decay back to their ground $S_{1/2}$ states. There are several decay channels, through the emission of either π-polarized or $\sigma^{\pm}$-polarized spontaneous emission photons [see Fig. 1(b)].
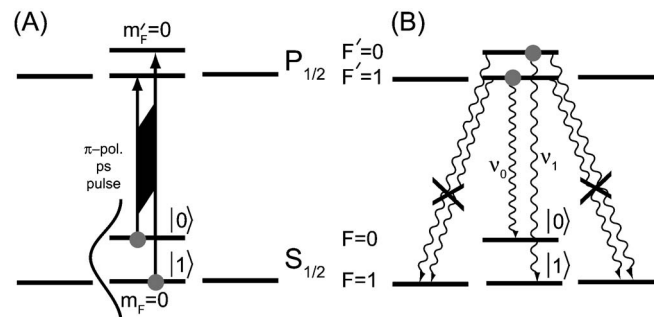

FIG. 1. The atomic level configuration and the laser excitation scheme. (a) An ultrafast laser pulse transfers the atomic qubit state from the ground levels to the excited levels. (b) The atom decays back to the ground levels, with the frequency of the spontaneously emitted photon correlated with the atomic qubit state (marked as the signal modes ν_0 and ν_1 in the figure). The photon from the $\sigma^{\pm}$ decay channels is filtered through polarization selection.

We first consider the decay channels with a π-polarized emission photon. In this case, the excited levels $|F'+1,m=0\rangle$ and $|F',m=0\rangle$ can only decay back to the ground states $|F,m=0\rangle$ and $|F+1,m=0\rangle$, respectively. While photons from these two decay channels have the same polarization, they have slightly different frequencies. The frequency difference is given by $\Delta_{HF}^S+\Delta_{HF}^P$, the sum of the hyperfine splittings of the ground $S_{1/2}$ and excited $P_{1/2}$ states. This frequency difference is typically much larger than the natural linewidth of the excited level [16], so the corresponding photons from the two π-decay channels are well resolved in frequency. This defines two frequency modes for the emitted photon field, and we call them the ν_0 and ν_1 modes, respectively. If the atom is initially in the qubit state $|\Psi_a\rangle=c_0|0\rangle+c_1|1\rangle$, then after this excitation-decay process the atom-photon system evolves to an entangled state

$$|\Psi_{ap}\rangle = c_0|0\rangle|\nu_0\rangle + c_1|1\rangle|\nu_1\rangle, \qquad (1)$$

if we only collect the photon from the π-decay channels, where $|\nu_0\rangle$ and $|\nu_1\rangle$ represent a single-photon state in the frequency modes ν_0 and ν_1, respectively. Any photon from the $\sigma^\pm$ decay channels is assumed to be blocked through a polarization filter. This result is somewhat similar to the previous demonstration of the atom-photon entanglement [4,5], but there are important differences. First, the final state $|\Psi_{ap}\rangle$ keeps track of the information c_0,c_1 of the initial qubit state. Thus, the scheme here is not just an entangling protocol [17,18], but is instead an entangling *gate* with the final quantum state depending on the initial state. As we will see later, this type of gate can form the basis for scalable quantum computation, and is therefore more powerful than merely an entangling operation. Second, the spontaneous emission photon with either frequency ν_0 or ν_1 has the same spatial mode, so good spatial mode matching of this photonic qubit is possible even if we increase the solid angle of collection. In the previous entangling protocol [4,5,17], the quantum information is carried by different polarization modes of the photon, which have different spatial emission patterns. This requires small collection solid angles in order to both maintain orthogonality and ensure adequate spatial matching of the photonic qubit states.

To perform a gate on two remote atoms, the spontaneous emission photons from the decay channels in each atom are collected in a certain solid angle, and directed onto a beam splitter for interference (see Fig. 2). The output of the beam splitter is measured by two single-photon detectors. We keep the resulting outcome atomic state only when we register a photon from each detector. In this case, what we have performed is a "measurement gate" on the atoms 1 and 2. It corresponds to a quantum nondemolition measurement of the operator Z_1Z_2, where Z_i (or X_i) stands for the z (or x) component of the Pauli matrix associated with atomic qubit i. After the coincidence measurement of photons on both detectors, the atomic state is projected to the eigenspace of Z_1Z_2 with -1 eigenvalue. To see this, we note that before the measurement, the state of both atom-photon systems can be written as $|\Psi_{ap}\rangle_1\otimes|\Psi_{ap}\rangle_2$, where $|\Psi_{ap}\rangle_1$ has the form of Eq. (1) and $|\Psi_{ap}\rangle_2$ can be written as $|\Psi_{ap}\rangle_2=d_0|0\rangle_2|\nu_0\rangle_2+d_1|1\rangle_2|\nu_1\rangle_2$. To register a photon from each detector, the two
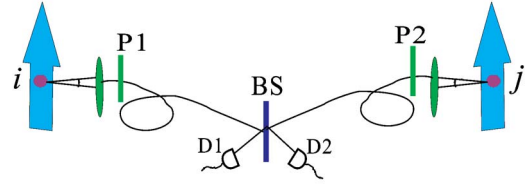

FIG. 2. (Color online) The ZZ measurement gate on the atoms i and j. The spontaneous emission photons from the π-decay channels of these two atoms are collected, interfered at the beam splitter (BS), and then detected by two single-photon detectors ($D1$ and $D2$). If each detector registers a photon, the atomic state is projected onto the eigenspace of the Z_iZ_j operator.

photons before the beam splitter need to go to different sides, which means they should be in the antisymmetric component $|\Phi_{AS}\rangle=(|\nu_0\rangle_1|\nu_1\rangle_2-|\nu_1\rangle_1|\nu_0\rangle_2)/\sqrt{2}$ (for photons in the symmetric states, they always go to the same detector). So, given that the photons take separate paths after the beam splitter, the state of the atoms 1,2 is given by the projection

$$\begin{aligned}|\Psi_{12}\rangle &\propto \langle\Phi_{AS}||\Psi_{ap}\rangle_1\otimes|\Psi_{ap}\rangle_2\\ &\propto c_0d_1|0\rangle_1|1\rangle_2-c_1d_0|1\rangle_1|0\rangle_2 \propto Z_1(I-Z_1Z_2)|\Psi_a\rangle_1\\ &\otimes|\Psi_a\rangle_2,\end{aligned} \qquad (2)$$

where $I-Z_1Z_2$ is the corresponding projector, and Z_1 is a trivial additional single-bit gate on atom 1, which we will neglect in the following. This measurement gate, of course, only succeeds with a finite probability. The overall success probability is given by $p_s=\eta_d^2\eta_c^2\eta_b^2/4$, where η_d is the quantum efficiency of each detector, η_c is the photon collection efficiency (proportional to the solid angle), and η_b is the branching ratio for the atom to decay along the π channel. We have an additional factor of $1/4$ in p_s describing the average probability for the two spontaneous emission photons to go to different detectors (averaged over all the possible initial atomic states). In the above contributions to the success probability, the collection efficiency is typically the smallest and thus dominates the overall efficiency. That is why it is important to increase the collection solid angle as much as possible. Alternatively, one can also increase this efficiency with the use of optical cavities surrounding the atoms [19]. The overall success probability p_s is typically small. For instance, for a ^{111}Cd$^+$ ion decaying from the $P_{3/2}$ state, the branching ratio into the π channel $\eta_b=2/3$, the photon collection efficiency $\eta_c\sim2\%$ in free space [4], and the detector efficiency $\eta_d\sim20\%$. This leads to an overall success probability $p_s\sim2\times10^{-6}$. If the collection efficiency is increased by a factor of 10 with a larger collection solid angle or with a surrounding cavity (not necessarily high finesse), the success probability will be significantly increased by a factor of 100.

The above measurement gate is robust to noise. We do not require that the atoms be localized to the Lamb-Dicke limit. In general, atomic motion occurs with a time scale of the trap frequency ν_t, typically much smaller than the decay rate γ of the excited atomic level. Thus, for each spontaneous emission pulse, we can safely assume the atom to be in a fixed

but random position $\mathbf{r}$. In this case, both of the frequency components $|\nu_0\rangle$ and $|\nu_1\rangle$ will acquire the same random phase factor proportional to $e^{i\mathbf{k}\cdot\mathbf{r}}$, where $\mathbf{k}$ is the wave vector associated with the spontaneous emission photon. This overall phase therefore has no effect on the resultant measurement gate as shown in Eq. (2). If we take into account the motion of the atom within the pulse duration, the pulse from this moving atom also has a slight Doppler shift $\delta\omega=\mathbf{k}\cdot\mathbf{v} \sim |\mathbf{k}|\nu_t l_s$ in its frequency, where $\mathbf{v}$ is the random atom velocity at that moment, and l_s is the characteristic length scale for the atom oscillation. We need this random Doppler shift to be significantly smaller than the bandwidth of the pulse in order to have a good shape matching of the spontaneous emission pulses from different atoms. So, there is a further requirement $|\mathbf{k}|\nu_t l_s \ll \gamma$, which is consistent with the assumption $\nu_t \ll \gamma$. Finally, this gate is also very insensitive to the birefringence and the phase drift in the optical interferometer. Both of the components $|\nu_0\rangle$ and $|\nu_1\rangle$ have the same polarization, and they are very close in frequency. So they essentially experience the same noisy phase shift under fluctuation of the optical path length, again canceling.

We have shown how to perform a probabilistic measurement gate on remote atoms by projecting the system state to the eigenspace of the Z_1Z_2 operator. Such a gate only succeeds with a small probability, but it is very robust to noise. This type of probabilistic gate can lead to efficient quantum computation, no matter how small the success probability p_s [6,7,20]. The proof is based on efficient construction of the two-dimensional (2D) cluster state, which has been shown to be a sufficient resource for universal quantum computation [21]. To construct a 2D cluster state of size n, the number of pulses (elementary operations) scales with n by $n \ln n$, and scales with the inverse of the gate success probability $1/p_s$ nearly polynomially. The exact scaling formula can be found in Ref. [6], where it is derived for the case of probabilistic controlled-phase-flip (CPF) gates. For the ZZ measurement gate, the scaling formula is almost the same. To see this, we can simply note the following two facts: (1) If one starts with two qubits (atoms) in the co-eigenstate of X_1 and X_2 (a product state), the final state after a ZZ measurement is projected

to a co-eigenstate of the stabilizer operators Z_1Z_2 and X_1X_2, which is equivalent to the two-qubit cluster state under single-bit rotations [7]; (2) assume that one has prepared two 1D cluster chains, each of n qubits. The stabilizer operators for the boundary qubits n and $n+1$ of the two chains are denoted by X_nZ_{n-1} and $X_{n+1}Z_{n+2}$, respectively. A ZZ measurement of these two boundary qubits generates the new stabilizer operators Z_nZ_{n+1} and $X_nX_{n+1}Z_{n-1}Z_{n+2}$. This operation actually connects the two chains into a cluster state of $2n-1$ qubits (the central qubits n and $n+1$ together represent one logic qubit with the encoded $X_L=X_nX_{n+1}$ and $Z_L=Z_n$ or Z_{n+1}). From these two facts, we can derive the recursion relations. Following the same argument as in the case for the CPF gate [6], we can show that starting with two cluster chains each of n qubits, the average length of the cluster state after this probabilistic measurement gate is given by $n'=\Sigma_i(2n-1-4i)p_s(1-p_s)^i \approx 2n-n_c$, where the critical length $n_c=1+4(1-p_s)/p_s$ and p_s is the gate success probability. Compared with the case of the CPF gate, the only difference is that the critical length n_c changes from $4(1-p_s)/p_s$ to $1+4(1-p_s)/p_s$, and such a change is negligible in the case of a small success probability with $4/p_s \gg 1$. So, for this ZZ measurement gate, we find nearly the same scaling formula derived in Ref. [6].

In summary, we have proposed a scheme for probabilistic gates on remote trapped atoms or ions in free space, based on interference of optical frequency qubits from the atomic spontaneous emission driven by ultrafast laser pulses. This gate scheme does not require localization of the atoms to the Lamb-Dicke limit, and is robust to practical phase noise in the optical interferometers. This type of probabilistic gate could lead to an alternative way for efficient quantum computation.

[1] L. M. Duan, M. D. Lukin, J. I. Cirac, and P. Zoller, Nature (London) **414**, 413 (2001).

[2] E. Knill, R. Laflamme, and G. Milburn, Nature (London) **409**, 46 (2001).

[3] A. Kuzmich *et al.*, Nature (London) **423**, 731 (2003); C. H. van der Wal *et al.*, Science **301**, 196 (2003).

[4] B. B. Blinov, D. L. Moehring, L.-M. Duan, and C. Monroe, Nature (London) **428**, 153 (2004).

[5] D. L. Moehring, M. J. Madsen, B. B. Blinov, and C. Monroe, Phys. Rev. Lett. **93**, 090410 (2004).

[6] L.-M. Duan and R. Raussendorf, Phys. Rev. Lett. **95**, 080503 (2005).

[7] S. D. Barrett and P. Kok, Phys. Rev. A **71**, 060310(R) (2005).

[8] B. Wang and L.-M. Duan, Phys. Rev. A **72**, 022320 (2005).

[9] Y. L. Lim *et al.*, Phys. Rev. A **73**, 012304 (2006); Y. L. Lim, A. Beige, and L. C. Kwek, Phys. Rev. Lett. **95**, 030505 (2005).

[10] M. J. Madsen *et al.*, e-print quant-ph/0603258.

[11] D. Stick *et al.*, Nat. Phys. **2**, 36 (2006); D. Kielpinski, C. Monroe, and D. J. Wineland, Nature (London) **417**, 709 (2002).

[12] S. Seidelin *et al.*, e-print quant-ph/0601173 (2006).

[13] L. Deslauriers *et al.*, e-print quant-ph/0602003 (2006).

[14] If an ultrafast laser pulse is not available, one can replace it by two phase-locked narrowband pulses which drives the $D1$ transitions $|F,m=0\rangle \rightarrow |F'+1,m=0\rangle$ and $|F+1,m=0\rangle \rightarrow |F',m=0\rangle$ $(F'=F)$, respectively.

[15] For ^{111}Cd$^+$ (or for any atoms with the nuclear spin $I=1/2$), one can also drive the $D2$ line $S_{1/2} \rightarrow P_{3/2}$, where the two corresponding hyperfine transitions are given by $|F,m=0\rangle$

$\rightarrow |F',m=0\rangle$ and $|F+1,m=0\rangle \rightarrow |F'+1,m=0\rangle$ with $F'=F+1$ (see Ref. [10]).

[16] For instance, for ^{133}Cs atoms or ^{111}Cd$^+$ ions, the hyperfine splitting is about 9 (14) GHz, while the natural linewidth of the excited level (the inverse of the lifetime) is around 5 (60) MHz. In both cases, the condition is well satisfied.

[17] L.-M. Duan, B. B. Blinov, D. L. Moehring, and C. Monroe, Quantum Inf. Comput. **4**, 165 (2004).

[18] L. M. Duan and H. J. Kimble, Phys. Rev. Lett. **90**, 253601 (2003); C. Simon and W. T. M. Irvine, *ibid.* **91**, 110405 (2003).

[19] J. McKeever, J. R. Buck, A. D. Boozer, and H. J. Kimble, Phys. Rev. Lett. **93**, 143601 (2004); P. Maunz *et al.*, Nature (London) **428**, 50 (2004); J. A. Sauer *et al.*, Phys. Rev. A **69**, 051804(R) (2004); G. Guthorlein *et al.*, Nature (London) **414**, 49 (2001); A. Mundt *et al.*, Phys. Rev. Lett. **89**, 103001

(2002).

[20] Note, however, that the noise model assumed in Ref. [7] is more restrictive. It assumes there that if a gate fails, states of the two target qubits are not destroyed, but instead, they are subject only to Z type of errors (without bit flips from $|0\rangle$ to $|1\rangle$, for instance). In our physical implementation, however, due to the existence of σ^{pm}-decay channels (which are always there for any realistic atoms), there is a significant probability of bit-flip errors when a gate fails. So, in the case of a gate failure, one needs to trace out the destroyed qubits. The noise model here is exactly the same as what is assumed in Ref. [6]. We can follow the contruction there to prove scalability under this kind of noise model.

[21] H. J. Briegel and R. Raussendorf, Phys. Rev. Lett. **86**, 910 (2001); R. Raussendorf and H. J. Briegel, *ibid.* **86**, 5188 (2001).